

Anomalous Hall signatures of nonsymmorphic nodal lines in doped chromium chalcospinel CuCr_2Se_4

Subhasis Samanta,¹ Gang Chen,^{2,3,*} and Heung-Sik Kim^{1,4,†}

¹*Department of Physics, Kangwon National University, Chuncheon 24341, Korea*

²*Department of Physics and Center of Theoretical and Computational Physics,
The University of Hong Kong, Pokfulam Road, Hong Kong, China*

³*State Key Laboratory of Surface Physics and Department of Physics, Fudan University, Shanghai 200433, China*

⁴*Institute for Accelerator Science, Kangwon National University, Chuncheon 24341, Korea*

An emerging phase of matter among the class of topological materials is nodal line semimetal, possessing symmetry-protected one-dimensional gapless lines at the (or close to) the Fermi level in k -space. When the k -dispersion of the nodal line is weak, van Hove singularities generated by the almost flat nodal lines may be prone to instabilities introduced by additional perturbations such as spin-orbit coupling or magnetism. Here, we study Cr-based ferromagnetic chalcospinel compound CuCr_2Se_4 (CCS) via first-principles electronic structure methods and reveal the true origin of its dissipationless anomalous Hall conductivity, which was not well understood previously. We find that CCS hosts nodal lines protected by nonsymmorphic symmetries, located in the vicinity of Fermi level, and that such nodal lines are the origin of the previously observed distinct behavior of the anomalous Hall signature in the presence of electron doping. The splitting of nodal line via spin-orbit coupling produces a large Berry curvature, which leads to a significant response in anomalous Hall conductivity. Upon electron doping via chemical substitution or gating, or rotation of magnetization via external magnetic field, steep change of anomalous Hall behavior occurs, which makes CCS a promising compound for low energy spintronics applications.

Dissipationless charge or spin transport has been a key concept in condensed matter physics because of realizations of low-power electronic and spintronic devices and long-time preservation of quantum information that it promises [1–4]. Dissipationless transport phenomena often originates from topology of electronic structures, and it has been a hallmark of various topologically nontrivial states of matter such as quantum anomalous and spin Hall phases [5, 6], or topological semimetals such as magnetic Weyl and nodal semimetals [7, 8].

Magnetic topological material, such as topological insulators doped with magnetic ions [9–11] or magnetic nodal semimetals [12–15], are promising candidate to realize dissipationless Hall transport in room-temperature conditions. In terms of practical applications, on the other hand, vanishing density of states in Weyl or Dirac semimetals at the Fermi level is not favorable for good transport properties. In this regard nodal line semimetals with weak momentum space dispersion, which can host van Hove singularities in the vicinity of Fermi level, thanks to the one-dimensional line of zero-energy modes with nonvanishing measure in the k -space, seems promising in realizing dissipationless Hall transport for practical device applications.

It was previously reported that a chalcospinel compound, CuCr_2Se_4 (CCS) doped with Br, shows dissipationless anomalous Hall transport that is unaffected by the doping-induced disorder [16, 17]. Soon after the experimental report it was suggested to be an electronic Berry phase effect [18, 19]. However, the origin of the sharp doping-induced sign change in the anomalous Hall conductivity, as observed both in experiment [16] and theory [19], has not been understood well. In light of recent advancements in topological band theory, we revisit the anomalous Hall response of the electron-

doped CCS and reveal its origin. We found that the Br-doped CCS in its ferromagnetic state ($T_C \simeq 430$ K) is a half-metallic nodal line semimetal, where the nodal degeneracy at the zone boundary is protected by nonsymmorphic symmetries in the absence of spin-orbit coupling (SOC). Inclusion of Cr and Se SOC slightly splits the nodal degeneracy, generating a substantial sign-changing anomalous Hall response under electron doping because of the nodal-line-induced finite density of states. It is further shown that, thanks to its weak magnetocrystalline anisotropy [20], Br-doped CuCr_2Se_4 may show huge response of anomalous Hall signatures under external magnetic fields. Thereby, it is expected that electron-doped CuCr_2Se_4 would become a promising platform for dissipationless charge and spin transport applications.

Methods: For this study we carried out electronic structure calculations within local density approximation (LDA) using Vienna *Ab-initio* Simulation Package (VASP) [21]. Detailed investigation of spin-orbit coupling and computation of anomalous Hall conductivity vector was performed using *ab-initio*-based tight-binding model constructed via Wannier function [22] method as implemented in WANNIER90 package [23] (for more details see Supplemental Material).

Band structure of CCS: CCS is a metallic ferrimagnet ($T_C = 430$ K) with a cubic symmetry (space group No. 227), where the ferromagnetic ordering of Cr high-spin moments mostly contributes to the net magnetization [24]. Band structures of CCS with and without spin-orbit coupling are shown in Fig. 1, where Cr t_{2g} - and Se p -like hole characters can be clearly seen in the metallic bands close to the Fermi level. Cu states are most located about 2 eV below the Fermi level and weakly contribute to the metallic states. Note that charge configurations of Cu and Cr are not exactly Cu^{+1} and Cr^{3+} , respectively, because of negative charge transfer from Se^{2+}

ions to Cr and Cu sites yielding the metallic behavior.

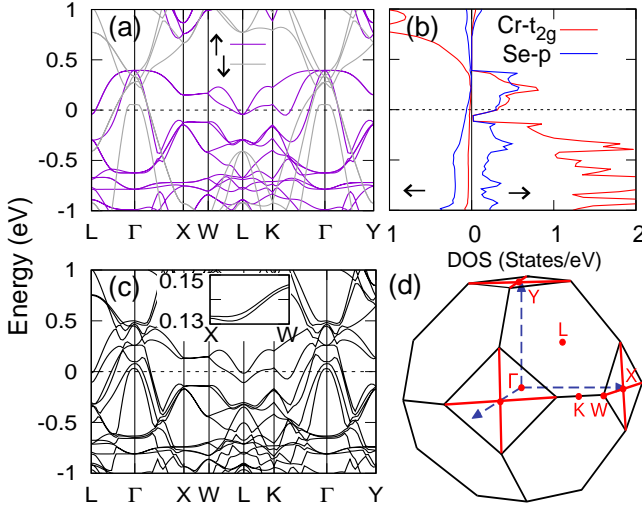


FIG. 1. Spin-polarized band structure and partial density of states (PDOS), obtained using (a)-(b) LDA and (c) LDA+SOC with magnetization direction parallel to [111]. PDOS clearly shows Van Hove singularities around Fermi level, where nodal lines are seen in the band structure. (d) First Brillouin zone of FCC lattice shows high symmetry points and paths of the nodal lines along X - W with thick red lines.

A salient feature of the CCS band structure is the presence of nearly flat two-fold degenerate bands in the majority spin channel (Fig. 1(a)), located close to the Fermi level (within the energy window $|E - E_F| \leq 0.15$ eV) on the X - W lines in the absence of spin-orbit coupling. These flat nodal lines induce van Hove singularities around ± 0.15 eV, as shown in the density of states plot (right panel in Fig. 1(a)), while dispersive minority spin channel almost does not contribute to the states close to the Fermi level (see Fig. 1(b)). These line degeneracies, namely the so-called Weyl nodal line features [25], are protected by two non-symmorphic and perpendicular d -glide planes that intersect on every X - W lines. Anticommutation relations between the two intersecting glide operations on the X - W lines enforce twofold degeneracy, which can be lifted with the loss of the glide symmetries via lattice distortions or spin-orbit coupling plus symmetry-breaking magnetism.

Indeed, Fig. 1(c) shows the band structure of CCS with including SOC and net magnetization parallel to the [111] direction. A small but finite splitting of the nodal lines on the X - W line is visible. The splitting persists when the magnetization direction is along [001] axis because the loss of glide plane. Orbital-projected density of states close to the nodal lines shows almost equal mixture of Cr t_{2g} and Se p -states (see right panels of Fig. 1(b)), so the splitting of the nodal lines can be attributed to the SOC of Cr d - and Se p -orbitals.

It has been well-known that splitting of nodal lines via SOC results in large intrinsic anomalous Hall signature and topological phases [15, 26]. Thanks to the flat dispersion of the

nodal line bands and the resulting finite density of states close to the Fermi level, SOC-induced anomalous Hall signatures in CCS should be significant. Furthermore, small SOC-induced splitting of the nodal lines in CCS may result in a sharp change of anomalous Hall character under charge doping as reported previously [16, 17].

Wannierized effective model and SOC: In order to investigate the role of SOC in anomalous Hall responses, we constructed a tight-binding (TB) Hamiltonian via Wannier orbital method [22, 27, 28]. Our Wannierized TB model incorporates 12 Cr- t_{2g} -like and 24 Se- p -like orbitals and faithfully represents nodal lines and other band features of majority spin channel close to the Fermi level (see Supplemental Material for more detail). Note that the contribution of the minority spin channel to the Hall conductivity should be marginal at most because of its negligibly small density of states (see Fig. 1(b)).

In the majority spin channel, where spin degree of freedom is frozen because of magnetic ordering, SOC behaves as an effective Zeeman field in the orbital sector; $\hat{H}_{\text{SO}} \rightarrow \hat{P}_{\mathbf{n}}^\dagger \hat{H}_{\text{SO}} \hat{P}_{\mathbf{n}} \simeq \frac{\hbar}{2} \sum_{\alpha} \lambda_{\alpha} \hat{L}_{\mathbf{n}}^{\alpha}$, where α is index for Cr and Se sites, $\hat{H}_{\text{SO}} \equiv \sum_{\alpha} \lambda_{\alpha} \hat{L}^{\alpha} \cdot \hat{S}^{\alpha}$ is original atomic SOC, \mathbf{n} is the magnetization direction, and $\hat{P}_{\mathbf{n}} \equiv \sum_{\alpha} |\uparrow_{\mathbf{n}}\rangle_{\alpha} \langle \uparrow_{\mathbf{n}}|_{\alpha}$ is a projection operator onto the majority spin channel along \mathbf{n} . Hence, SOC on top of nonzero magnetization along \mathbf{n} splits degeneracy between nonzero $L_{\mathbf{n}}$ states, which consist of nodal gapless lines at zone boundaries.

Anomalous Hall conductivity: To investigate anomalous Hall responses with respect to net magnetization direction in CCS, we employed Fukui-Hatsugai-Suzuki method to compute Berry curvature vector $\mathbf{\Omega}(\mathbf{k}) \equiv (\Omega_{yz}, \Omega_{xz}, \Omega_{xy})$ (\mathbf{k}) and anomalous Hall conductivities in a $80 \times 80 \times 80$ discretized k -space [29]. Two magnetization directions, [001] and [111] with respect to the cubic axes, were considered. Both Cr ($\lambda_{\text{Cr}}=0.02$ eV) and Se SOC ($\lambda_{\text{Se}}=0.05$ eV) were included, where values of λ_{Cr} and λ_{Se} were chosen to best fit the energy splitting of two bands close to the Fermi level at L point. Note that the Berry curvature vector $\mathbf{\Omega}(\mathbf{k})$ becomes identically zero at all k -point in the absence of SOC because of coexistence of the complex conjugation (*i.e.* product of time-reversal and global spin rotation operations) and inversion symmetries.

Figure 2 shows the effect of spin-orbit coupling on the Wannier TB band structure with different magnetization directions and the resulting anomalous Hall responses. Here, the inclusion of SOC unlocks two conditions necessary for finite anomalous Hall responses; first, as mentioned above, SOC splits nodal line degeneracies by coupling magnetization and band structure so that glide symmetries are lost except ones perpendicular to the magnetization direction. Second, because the global spin rotation symmetry is lost due to SOC, the complex conjugation symmetry which enforces $\mathbf{\Omega}(-\mathbf{k}) = -\mathbf{\Omega}(\mathbf{k})$, is gone. Hence, a finite anomalous Hall response that does not vanish under the k -summation emerges from the splitting of the nodal lines via SOC.

In the presence of SOC, bands along the high symme-

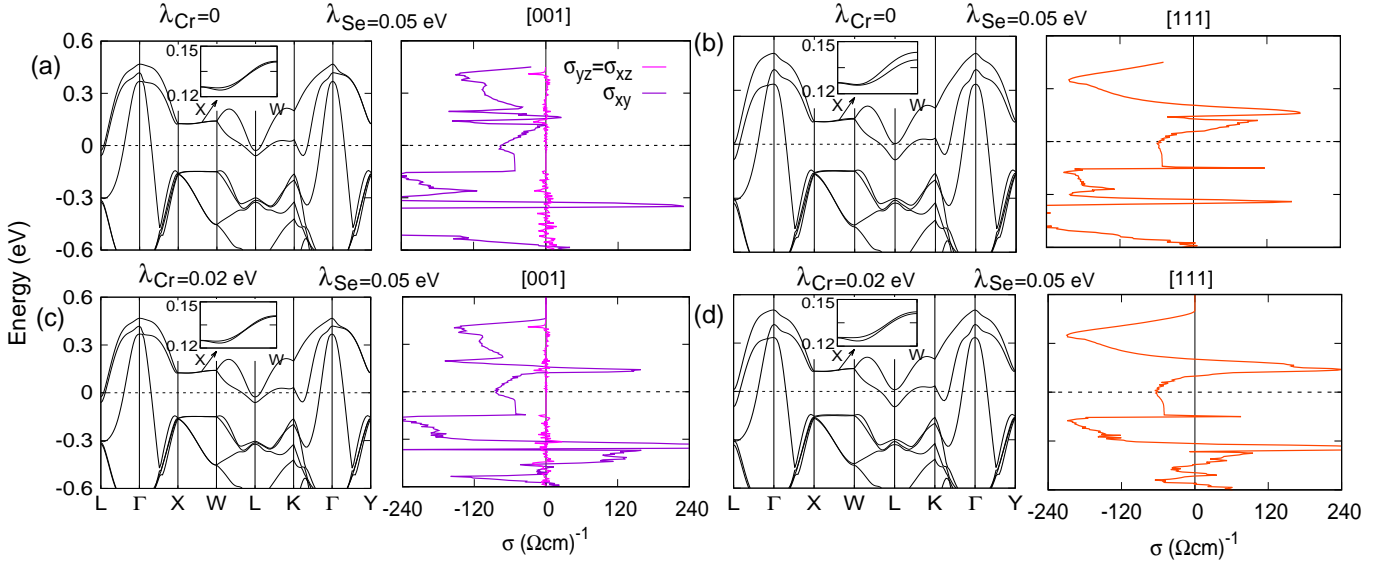


FIG. 2. (a)-(d) Band structure in the majority spin channel, obtained from TB Wannier model. The figures demonstrate the effect of Cr and Se spin-orbit couplings with two magnetization directions along [001] and [111]. Corresponding anomalous Hall conductivity shows a large enhancement in magnitude around nodal line in the electron doped region due to the splitting by spin-orbit couplings. The result suggests that Hall conductivity depends on both magnetization direction as well as spin-orbit coupling constants. Noisy features of $\sigma_{yz,xz}$ in right panels of (a) and (c) are from numerical noises that vanish in the limit of infinitely dense k -grid.A

try path X - W in Fig. 2 reveals several important features of the nodal line. Here, magnetization direction and spin-orbit coupling constants control the magnitude of the splitting. The SOC induced splitting energy along the nodal lines is marginal, of the order of few meV. In the case of [111] direction, splitting is more pronounced, and also, the role is λ_{Cr} is quite clear. The inclusion of λ_{Cr} effectively lowers the nodal line splitting. Since nodal line bands consist of hybridized Cr- t_{2g} - Se- p orbitals, net splitting reduces at W point due to the opposite parity of Cr and Se states. The nodal line too splits at X point, but its magnitude is negligibly small.

Anomalous Hall conductivities $\sigma(\mu)$ as a function of chemical potential μ is shown in Fig. 2 alongside band plots, where changes in $\sigma(\mu)$ introduced by the presence of Cr SOC and tilting of magnetization direction from [001] to [111] are shown. Note that anomalous Hall vectors behave in the same way as magnetic moments under symmetry operations, and four-fold and three-fold rotation symmetries remain unbroken in the cases of $\mathbf{M} // [001]$ and [111], respectively. Therefore, components of anomalous Hall vectors that are perpendicular to the magnetization cancel out, and only components parallel to the magnetization directions (σ_{xy} when $\mathbf{M} // [001]$, and $\sigma_{xy} = \sigma_{xz} = \sigma_{yz}$ when $\mathbf{M} // [111]$) survive, as shown in Fig. 2. In both cases of $\mathbf{M} // [001]$ and [111], a steep change in Hall conductivity is observed close to the nodal line when λ_{Cr} is included. As mentioned above, inclusion of λ_{Cr} narrows the gap and hence, there is a sharp change in magnitude of $\sigma(\mu)$. The result also suggests that both magnetization direction and SOC on both Cr and Se are equally important in order to observe a flarge change in anomalous Hall response close to the nodal lines in the electron-doped regime.

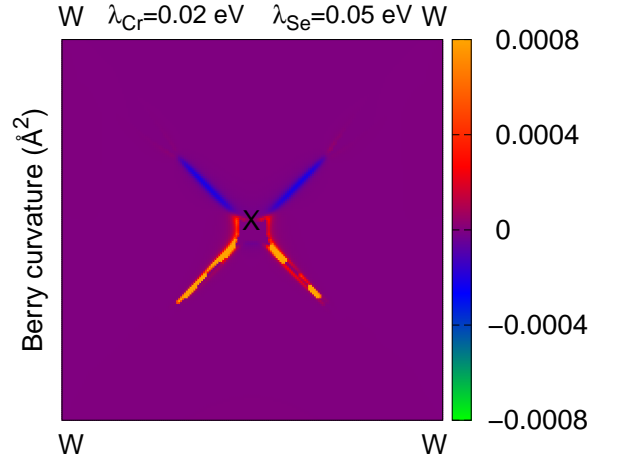


FIG. 3. Spin-orbit coupling splits the nodal line, resulting a large change in Berry Curvature observed along the X - W lines. This gives rise to a steep increase in magnitude of anomalous conductivity. Note, plot is obtained for $\mu = 0.125$ eV with $\mathbf{M} // [111]$.

In order to figure out the origin of large AHC in the electron doped region, in Fig. 3 we plotted the Berry curvature $\Omega_{xy}(\mathbf{k})$ on one square face of the first Brillouin zone containing X and W points when the magnetization is along [111] direction (*i.e.* $\Omega_{xy}(\mathbf{k}) = \Omega_{xz}(\mathbf{k}) = \Omega_{yz}(\mathbf{k})$) with $\mu = 0.125$ eV. Fig. 3 shows that the Berry curvature is concentrated on the X - W nodal lines, consistent with a previous theoretical finding [19].

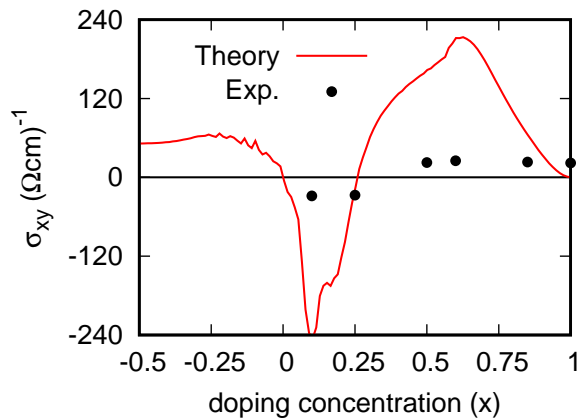


FIG. 4. Hall conductivity, plotted as a function of doping. For comparison, experimental Hall conductivity, adopted from the reference [16] for specific doping ($x = 0.1, 0.25, 0.5, 0.6, 0.85, 1$) concentration, are shown with filled circles. Our result explains the sign reversal behavior of the Hall signature.

It is noted that, with the presence of SOC, the loss of time-reversal symmetry causes an imbalance of Berry Curvature at \mathbf{k} and $-\mathbf{k}$ points with respect to the X point and the resulting nonzero net anomalous Hall conductivity.

Figure 4 shows computed $\sigma_{xy}(x)$ as a function of electron doping per formula unit x when $M//[111]$. Previous experimental Hall conductivity [16] for few selective doping concentrations is also displayed in the figure for comparison. The Hall response is maximum when doping concentration is close to 0.1. The sign change behavior is captured around $x=0.25$. Origin of experimental σ_{xy} close to $x=1$ should be more complicated due to effects from minority-spin bands or impurity scattering, whose contributions are absent in our Wannierized model.

Potential on-site correlation effects: In the splitting of nodal lines and resulting anomalous Hall effect in CuCr_2Se_4 , the role of Cr atomic Hund's coupling that gives rise to $S = 3/2$ Cr local moments, is crucial. After the Cr-moment-based ferromagnetism occurs, electronic structure calculation results within density functional theory provide a good agreement with experimental observations. However, it always remains to be a valid question whether other parts of Coulomb correlations, such as on-site repulsion, might play a significant role even in metallic systems. To better understand the effect of on-site Coulomb repulsion at Cr sites, we have performed DFT+ U [30] and DFT+DMFT (dynamical mean-field theory) [31, 32] calculations and presented our results in the Supplemental Material [33]. Therein, it is shown that *i*) DFT+ U tends to drive this system away from half-metallic regime, which is inconsistent with experimental observations of strong half-metallicity in this compound [24, 34] and that *ii*) the nearly-flat nodal line features remain stable under the effect

of dynamic on-site correlations within DFT+DMFT. We conclude that the presence of on-site electron correlations does not change our overall conclusion, and therefore suggest that our finding of nodal-line-induced anomalous Hall signatures in doped CuCr_2Se_4 is relevant to previous experimental findings [16, 17].

Discussion and summary: The substantial change in anomalous Hall conductivity between [001] and [111] near nodal lines reveal that the direction of magnetization plays a key role in tuning a large response. In addition, according to our density functional theory calculations, energy difference between [001] and [111] FM magnetization directions is found to be very small, 0.098 meV per formula unit (f.u.). This is mostly due to the relatively weak spin-orbit coupling constants at Cr atoms and the basal cubic symmetry. Earlier experimental studies show first and second order anisotropy constants to be of the same order ($K_1=0.084$ and $K_2=0.011$ meV/f.u.), consistent with our finding [20]. Hence, a not-too-strong external magnetic field of less than a Tesla may easily switch the magnetization direction and induce huge anomalous Hall response in this system.

In conclusion, we explain the origin of large anomalous Hall behavior in the doped CuCr_2Se_4 . Our analysis reveals that doubly degenerate nodal line along $X-W$ in the vicinity of Fermi-level is responsible for a large Hall signature. In the presence of spin-orbit coupling, splitting of nodal lines produces a non-zero Berry curvature along $X-W$, resulting in a large change in anomalous Hall response. In addition, weak magnetocrystalline anisotropy in CuCr_2Se_4 is favorable because it facilitates the switching of the magnetization direction and the resulting anomalous Hall conductivity with the application of an external magnetic field. With these, doped CuCr_2Se_4 becomes a promising candidate for studying magnetic topological semimetals and realizing low-power dissipationless spintronics applications.

Acknowledgements. S. Samanta was funded by the Korea Research Fellow (KRF) Program of the National Research Foundation of Korea (Grant No. 2019H1D3A1A01102984), and also thanks the National Supercomputing Center of Korea for providing computational resources including technical assistance (Grant No. KSC-2020-CRE-0156). HSK acknowledges the support of the National Research Foundation of Korea (Basic Science Research Program, Grant No. 2020R1C1C1005900). GC was supported by the Ministry of Science and Technology of China with Grants No. 2018YFE0103200, 2016YFA0300500, 2016YFA0301001, and by the Shanghai Municipal Science and Technology Major Project with Grant No. 2019SHZDZX01, and by the Research Grants Council of Hong Kong with General Research Fund with Grants No. 17303819.

* gchen_physics@fudan.edu.cn
† heungsikim@kangwon.ac.kr

- [1] Shuichi Murakami, Naoto Nagaosa, and Shou-Cheng Zhang, “Dissipationless quantum spin current at room temperature,” *Science* **301**, 1348–1351 (2003).
- [2] Dimitrie Culcer, Aydın Cem Keser, Yongqing Li, and Grigory Tkachov, “Transport in two-dimensional topological materials: recent developments in experiment and theory,” *2D Mater* **7**, 022007 (2020).
- [3] Ke He, Yayu Wang, and Qi-Kun Xue, “Topological materials: Quantum anomalous hall system,” *Annu. Rev. Condens. Matter Phys.* **9**, 329–344 (2018).
- [4] Yoshinori Tokura, Kenji Yasuda, and Atsushi Tsukazaki, “Magnetic topological insulators,” *Nat. Rev. Phys.* **1**, 126–143 (2019).
- [5] Naoto Nagaosa, Jairo Sinova, Shigeki Onoda, A. H. MacDonald, and N. P. Ong, “Anomalous hall effect,” *Rev. Mod. Phys.* **82**, 1539–1592 (2010).
- [6] M. Z. Hasan and C. L. Kane, “Colloquium: Topological insulators,” *Rev. Mod. Phys.* **82**, 3045–3067 (2010).
- [7] Xiangang Wan, Ari M. Turner, Ashvin Vishwanath, and Sergey Y. Savrasov, “Topological semimetal and fermi-arc surface states in the electronic structure of pyrochlore iridates,” *Phys. Rev. B* **83**, 205101 (2011).
- [8] Kai-Yu Yang, Yuan-Ming Lu, and Ying Ran, “Quantum hall effects in a weyl semimetal: Possible application in pyrochlore iridates,” *Phys. Rev. B* **84**, 075129 (2011).
- [9] Rui Yu, Wei Zhang, Hai-Jun Zhang, Shou-Cheng Zhang, Xi Dai, and Zhong Fang, “Quantized anomalous hall effect in magnetic topological insulators,” *Science* **329**, 61–64 (2010).
- [10] Cui-Zu Chang, Jinsong Zhang, Xiao Feng, Jie Shen, Zuocheng Zhang, Minghua Guo, Kang Li, Yunbo Ou, Pang Wei, Li-Li Wang, Zhong-Qing Ji, Yang Feng, Shuaihua Ji, Xi Chen, Jinfeng Jia, Xi Dai, Zhong Fang, Shou-Cheng Zhang, Ke He, Yayu Wang, Li Lu, Xu-Cun Ma, and Qi-Kun Xue, “Experimental observation of the quantum anomalous hall effect in a magnetic topological insulator,” *Science* **340**, 167–170 (2013).
- [11] Cui-Zu Chang, Weiwei Zhao, Duk Y. Kim, Haijun Zhang, Badih A. Assaf, Don Heiman, Shou-Cheng Zhang, Chaoxing Liu, Moses H. W. Chan, and Jagadeesh S. Moodera, “High-precision realization of robust quantum anomalous hall state in a hard ferromagnetic topological insulator,” *Nat. Mater.* **14**, 473–477 (2015).
- [12] Gang Xu, Hongming Weng, Zhijun Wang, Xi Dai, and Zhong Fang, “Chern semimetal and the quantized anomalous hall effect in HgCr_2Se_4 ,” *Phys. Rev. Lett.* **107**, 186806 (2011).
- [13] Zhijun Wang, M. G. Vergniory, S. Kushwaha, Max Hirschberger, E. V. Chulkov, A. Ernst, N. P. Ong, Robert J. Cava, and B. Andrei Bernevig, “Time-reversal-breaking weyl fermions in magnetic heusler alloys,” *Phys. Rev. Lett.* **117**, 236401 (2016).
- [14] Satoru Nakatsuji, Naoki Kiyohara, and Tomoya Higo, “Large anomalous hall effect in a non-collinear antiferromagnet at room temperature,” *Nature* **527**, 212–215 (2015).
- [15] Kyoo Kim, Junho Seo, Eunwoo Lee, K.-T. Ko, B. S. Kim, Bo Gyu Jang, Jong Mok Ok, Jinwon Lee, Youn Jung Jo, Woun Kang, Ji Hoon Shim, C. Kim, Han Woong Yeom, Byung II Min, Bohm-Jung Yang, and Jun Sung Kim, “Large anomalous hall current induced by topological nodal lines in a ferromagnetic van der waals semimetal,” *Nat Mater* **17**, 794–799 (2018).
- [16] Wei-Li Lee, Satoshi Watauchi, V. L. Miller, R. J. Cava, and N. P. Ong, “Dissipationless anomalous hall current in the ferromagnetic spinel $\text{CuCr}_2\text{Se}_{4-x}\text{Br}_x$,” *Science* **303**, 1647–1649 (2004).
- [17] Wei-Li Lee, S. Watauchi, V. L. Miller, R. J. Cava, and N. P. Ong, “Anomalous hall heat current and nernst effect in the $\text{CuCr}_2\text{Se}_{4-x}\text{Br}_x$ ferromagnet,” *Phys. Rev. Lett.* **93**, 226601 (2004).
- [18] Di Xiao, Yugui Yao, Zhong Fang, and Qian Niu, “Berry-phase effect in anomalous thermoelectric transport,” *Phys. Rev. Lett.* **97**, 026603 (2006).
- [19] Yugui Yao, Yongcheng Liang, Di Xiao, Qian Niu, Shun-Qing Shen, X. Dai, and Zhong Fang, “Theoretical evidence of the berry-phase mechanism in anomalous hall transport: First-principles studies of $\text{CuCr}_2\text{Se}_{4-x}\text{Br}_x$,” *Phys. Rev. B* **75**, 020401 (2007).
- [20] I. Nakatani, H. Nose, and K. Masumoto, “Magnetic properties of CuCr_2Se_4 single crystals,” *J. Phys. Chem. Solids* **39**, 743–749 (1978).
- [21] G. Kresse and J. Furthmüller, “Efficient iterative schemes for ab initio total-energy calculations using a plane-wave basis set,” *Phys. Rev. B* **54**, 11169–11186 (1996).
- [22] Ivo Souza, Nicola Marzari, and David Vanderbilt, “Maximally localized wannier functions for entangled energy bands,” *Phys. Rev. B* **65**, 035109 (2001).
- [23] Giovanni Pizzi, Valerio Vitale, Ryotaro Arita, Stefan Blögel, Frank Freimuth, Guillaume Géranton, Marco Gibertini, Dominik Gresch, Charles Johnson, Takashi Koretsune, Julien Ibañez-Azpiroz, Hyungjun Lee, Jae-Mo Lihm, Daniel Marchand, Antimo Marrazzo, Yuriy Mokrousov, Jamal I Mustafa, Yoshiro Nohara, Yusuke Nomura, Lorenzo Paulatto, Samuel Poncé, Thomas Ponweiser, Junfeng Qiao, Florian Thöle, Stepan S Tsirkin, Małgorzata Wierzbowska, Nicola Marzari, David Vanderbilt, Ivo Souza, Arash A Mostofi, and Jonathan R Yates, “Wannier90 as a community code: new features and applications,” *J. Phys.: Condens Matter* **32**, 165902 (2020).
- [24] A. Kimura, J. Matsuno, J. Okabayashi, A. Fujimori, T. Shishidou, E. Kulatov, and T. Kanomata, “Soft x-ray magnetic circular dichroism study of the ferromagnetic spinel-type Cr chalcogenides,” *Phys. Rev. B* **63**, 224420 (2001).
- [25] Baojie Feng, Run-Wu Zhang, Ya Feng, Botao Fu, Shilong Wu, Koji Miyamoto, Shaolong He, Lan Chen, Kehui Wu, Kenya Shimada, Taichi Okuda, and Yugui Yao, “Discovery of weyl nodal lines in a single-layer ferromagnet,” *Phys. Rev. Lett.* **123**, 116401 (2019).
- [26] Youngkuk Kim, Benjamin J. Wieder, C. L. Kane, and Andrew M. Rappe, “Dirac line nodes in inversion-symmetric crystals,” *Phys. Rev. Lett.* **115**, 036806 (2015).
- [27] Nicola Marzari and David Vanderbilt, “Maximally localized generalized wannier functions for composite energy bands,” *Phys. Rev. B* **56**, 12847–12865 (1997).
- [28] Hongming Weng, Taisuke Ozaki, and Kiyoyuki Terakura, “Revisiting magnetic coupling in transition-metal-benzene complexes with maximally localized wannier functions,” *Phys. Rev. B* **79**, 235118 (2009).
- [29] Takahiro Fukui, Yasuhiro Hatsugai, and Hiroshi Suzuki, “Chern numbers in discretized brillouin zone: Efficient method of computing (spin) hall conductances,” *J. Phys. Soc. Jpn.* **74**, 1674–1677 (2005).
- [30] S. L. Dudarev, G. A. Botton, S. Y. Savrasov, C. J. Humphreys, and A. P. Sutton, “Electron-energy-loss spectra and the structural stability of nickel oxide: An LSDA+U study,” *Phys. Rev. B* **57**, 1505–1509 (1998).
- [31] Kristjan Haule, Chuck-Hou Yee, and Kyoo Kim, “Dynamical mean-field theory within the full-potential methods: Electronic structure of CeIrIn_5 , CeCoIn_5 , and CeRhIn_5 ,” *Phys. Rev. B* **81**, 195107 (2010).
- [32] Kristjan Haule, “Structural predictions for correlated electron materials using the functional dynamical mean field theory approach,” *J. Phys. Soc. Jpn.* **87**, 041005 (2018).

[33] For more details please refer to the Supplemental Material.

[34] Aniruddha Deb, M. Ito, V. Tsurkan, and Y. Sakurai, “Effect of substitution of Cl and Br for Se in the ferromag-

netic spinel CuCr_2Se_4 : A magnetic Compton profile study,” [Phys. Rev. B **75**, 024413 \(2007\)](#).